Ultraconfined Interlaced Plasmons

Tiago A. Morgado,* João S. Marcos, Mário G. Silveirinha,† and Stanislav I. Maslovski

Department of Electrical Engineering, Instituto de Telecomunicações, University of Coimbra, 3030 Coimbra, Portugal

(Received 4 January 2011; published 3 August 2011)

We describe a mesoscopic excitation in strongly coupled grids of metallic nanorods, resulting from the hybridization of weakly bounded plasmons. It is shown both theoretically and experimentally that the characteristic spatial scale of the interlaced plasmons is determined by geometrical features, rather than from the electrical length of the nanorods, and that due to their wide band nature, weak sensitivity to metallic absorption, and subwavelength mode sizes, such plasmons may have exciting applications in waveguiding in the nanoscale.

DOI: 10.1103/PhysRevLett.107.063903 PACS numbers: 42.70.Qs, 41.20.Jb, 78.20.Ci, 78.66.Sq

Nanoplasmonics has important applications in sensing, nanoscopy, and recently has attracted attention due to its potential in cancer therapy [1]. Because of the extreme subwavelength nature of the plasmon field, the coupling between quantum emitters and plasmonic waveguides may have an efficiency close to unity, and hence plasmons are the basis for novel quantum generators and nanoscale amplifiers. Moreover, plasmons can effectively mediate the entanglement of quantum bits, and this can lead to the test of fundamental aspects in quantum information science [2].

These exciting applications are made possible by surface plasmon polaritons (SPPs), i.e., charge density waves supported by metal-dielectric interfaces [3]. The regime of strong confinement is viable at optical frequencies where the dielectric constant of metals is predominantly real and negative. At lower frequencies, metals begin resembling perfect electric conductors (PECs), leading to weakly bounded SPPs. One option to overcome this limitation at terahertz frequencies is to use doped semiconductors instead of metals [4]. However, the effect of loss may hinder practical applications. Yet, another possibility to mimic SPPs requires tailoring metal surfaces with subwavelength corrugations, and is based on spoof plasmons [5–9]. Despite the strong field confinement provided by spoof plasmons, they typically have a narrowband electromagnetic response.

In this Letter, we show that the answer to broadband ultrasubwavelength waveguiding at terahertz and infrared frequencies may lie on strongly coupled interlaced charge density waves, whose characteristic spatial period of oscillations is determined by the geometry, rather from the electron concentration in the metal or the electrical length of the metal structures. To begin with, let us revisit the waveguiding properties of a cylindrical metallic rod oriented along the z direction. The fundamental guided mode supported by the rod is a transverse magnetic (TM) mode with electric field components E_z and E_r, independent of the azimuthal coordinate φ [3]. Unless the permittivity of the metal satisfies $\varepsilon_m \sim -\varepsilon_0$, as in the optical domain, this TM mode is very weakly bounded to the rod and $|E_z| \ll |E_r|$. A greater confinement may be obtained by corrugating the metallic wire, exciting in this manner spoof plasmons [5]. In simple physical terms, this can be understood by noting that a corrugated wire may be seen as a set of coupled cavities (resonators). Each resonator is associated with a groove whose wavelength of resonance is about $\lambda \approx 4h$, where h is the depth of the groove. When the driving frequency is close to the resonance, the cavities are very strongly coupled by evanescent fields leaking out from them, and consequently an excitation can be propagated closely attached to the corrugated rod (spoof plasmon). Nevertheless, this phenomenon is resonant and extremely narrowband. Moreover, even at resonance, the overall diameter of the corrugated wire is roughly $2R \approx \lambda/2$, which contrasts markedly with the ultrasubwavelength sizes of plasmonic wires at optical frequencies.

To further illustrate the difficulties of waveguiding in a subwavelength scale, let us consider an array of metallic wires with no corrugations, instead of a single continuous corrugated wire. Specifically, we examine a wire medium slab with thickness L, being all the wires perpendicular to the interfaces at $z = 0$ and $z = L$ [top inset of Fig. 1(a)]. The array period is a, and we are interested in propagation along the x direction with propagation constant k_x. Figure 1(a) shows the dispersion of the fundamental guided mode (with field components E_x, E_z, and H_y), numerically calculated assuming perfectly conducting (PEC) wires. For a comparison, we also plot in Fig. 1(a) the dispersion diagram of the spoof plasmons supported by a corrugated wire with typical geometrical parameters, obtained using Eq. (3) of Ref. [5]. As seen, both waveguides enable a strong confinement, but only when the characteristic size of the waveguide is about $\lambda/2$. This is not really surprising since these strongly confined modes are rooted in the same physical mechanism in both cases. Indeed, in the wire medium slab each metallic wire may be regarded as a resonator (with resonant wavelength equal to $\lambda = 2L$ for

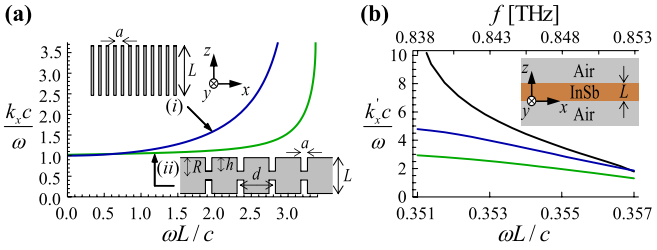

FIG. 1 (color online). (a) Normalized propagation constant k_x of the fundamental guided mode as a function of the frequency for (i) an array of metallic wires (blue upper curve) ($a = L/10$ and the radius of the wires is $r_w = 0.05a$), and (ii) a corrugated metallic wire (green lower curve) ($a = 10$ μm, $d = 50$ μm, $R = 100$ μm, $h = 65$ μm, and $L = 2R$). (b) Real part of the normalized propagation constant k_x' of the even TM-polarized guided mode as a function of the frequency for a InSb slab waveguide in air with thickness $L = 20$ μm. The permittivity of the semiconductor at 225 K is described by the Drude model with $\varepsilon_\infty = 15.7$ and $\omega_p/2\pi = 3.42$ THz [4]. Black curve: $\Gamma/\omega_p = 0$; blue (dark gray) curve: $\Gamma/\omega_p = 0.005$; green (light gray) curve: $\Gamma/\omega_p = 0.01$.

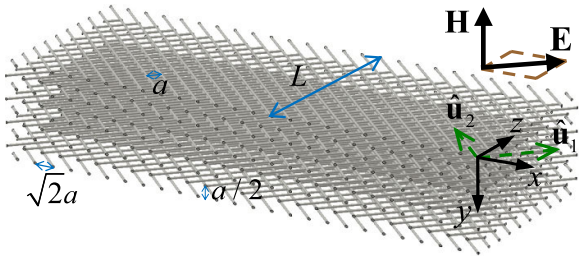

FIG. 2 (color online). (a) Two wire meshes are geometrically entangled resulting in the hybridization of the weakly bounded plasmons supported by each of them. The structure is formed by two sets of parallel wires arranged in square lattices with lattice constant a. The wires are embedded in a dielectric with relative permittivity ε_h.

metals with high conductivity), and, similar to the corrugated wire, when $\lambda \approx 2L$ the resonators are strongly coupled by evanescent field tails.

How can we overcome these apparently fundamental limitations? As shown next, an option is to force the plasmons to strongly interact on a length scale not determined by the wavelength of light. To see how this can be done, consider again the wire medium slab described before. From a macroscopic perspective (after some spatial averaging is considered) the only nonzero electric field components associated with the guided mode propagating along the x direction are E_x and E_z. Moreover, since the tangential electric field at the metallic wires is weak, for long wavelengths the dominant (macroscopic) field component is E_x. Let us now suppose that all the wires are rotated by -45° around the y axis, so that they become parallel to the unit vector $\hat{\mathbf{u}}_1 = (1, 0, 1)/\sqrt{2}$. In this scenario, nothing particularly exciting happens, except that the dominant component of the electric field is no longer E_x, but instead it is the projection of the electric field on $\hat{\mathbf{u}}_2 = (-1, 0, 1)/\sqrt{2}$. However, something really dramatic happens if we entangle two of such tilted wire medium slabs, with wires oriented along perpendicular directions. Specifically, we want to consider a crossed wire mesh such that the planes $y = la$ contain wires oriented along $\hat{\mathbf{u}}_1$, and the planes $y = la + a/2$ contain wires oriented along $\hat{\mathbf{u}}_2$, where l is an integer number (Fig. 2). This "double wire medium" has been considered in some previous works in different contexts [10,11]. What is really peculiar about this structure is that the wire mesh formed by wires oriented along $\hat{\mathbf{u}}_1$ creates an electric field mainly oriented along the direction $\hat{\mathbf{u}}_2$, which is thus strongly interacting with the wire mesh oriented along $\hat{\mathbf{u}}_2$, and vice versa. Thus, each wire mesh effectively blocks the electric field created by the currents flowing in the complementary wire mesh, and thus effectively repels the electric field away forcing fluctuations of the charge density in a subwavelength scale, and thus a strong confinement of the associated fields. This enables a mesoscopic excitation designated here as "interlaced plasmon pair" to emphasize that its physical origin is rooted on the geometrical entanglement of the charge density waves supported by perpendicular wire dipoles. A recent paper [8], also reported improved field confinement due to the hybridization of spoof plasmons. However, such a solution is relatively narrowband, and is based on the resonant response of SiC in the infrared range.

Even though a few layers of wires are sufficient to obtain a strong field confinement, first we consider the case of a slab with thickness L formed by an infinite number of crossed wire planes, stacked along the y direction (Fig. 2). Figure 3(a) depicts the dispersion characteristic of the interlaced plasmons for a fixed substrate thickness L and different densities of wires a/L. The results (discrete symbols) were calculated with the eigenmode solver of CST Microwave Studio. We have as well calculated the dispersion characteristic of the guided modes analytically (with macroscopic fields components H_y, E_x, and E_z) using the effective medium model of the double wire medium [solid curves in Fig. 3(a)], taking into account the effects of spatial dispersion and additional boundary conditions, as explained in detail in the Supplemental Material [12].

As seen in Fig. 3(a), the considered slab has an exotic and intriguing dispersion diagram, where it stands out the peculiar entanglement of the different branches of the dispersion characteristic, very different from the dispersion diagrams of either dielectric or metal based planar waveguides. The guided modes are highly confined (with $k_x c/\omega \gg 1$) even when the thickness L of the waveguide is ultrasubwavelength ($L/\lambda \leq 1/10$). This occurs, for example, in Fig. 3(a) (ii) for frequencies larger than $\omega L/c \approx 0.5$ as well as in Fig. 3(a)(iii) for frequencies larger than $\omega L/c \approx 0.4$, extending over a wide frequency band. Since the spatial period of oscillations of the interlaced plasmons is mainly determined by the lattice constant of the wire grids, the degree of confinement can be enhanced by increasing the density of

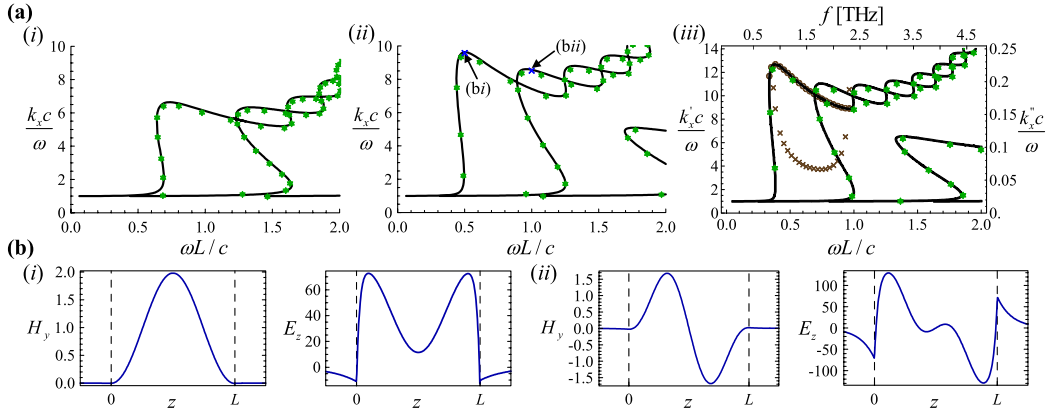

FIG. 3 (color online). (a) Normalized propagation constant $k_x = k_x' + ik_x''$ of the interlaced plasmons as a function of the normalized frequency, for a fixed waveguide thickness L and different lattice periods a. The radius of the wires is $r_w = 0.05a$. (i) $a = L/10$, (ii) $a = L/15$, and (iii) $a = L/20$. The (black) solid curves and the (green or gray) discrete symbols correspond to PEC wires ($k_x'' = 0$) and are obtained from the homogenization model [12] and CST Microwave Studio simulations, respectively. The circles and crosses in (iii) represent k_x' and k_x'', respectively, for a waveguide with thickness $L = 20$ μm and wires made of Ag. (b) Profiles of $H_y[A/m]$ and $E_z[V/m]$; (i) and (ii) correspond to the points (bi) and (bii) of (a)(ii).

wires, i.e., by reducing a/L, even if the metal volume fraction is kept fixed [see Fig. 3(a)(i)–(iii)]. Notice that the fields in the air regions decay with the attenuation constant $\gamma_0 = (\omega/c)\sqrt{(k_x c/\omega)^2 - 1}$, and thus the characteristic decay length in the transverse direction can be a tiny fraction of the wavelength in free space. This is illustrated in Fig. 3(b) (based on the analytical model [12]), which represents the transverse field distributions of the guided modes for the points marked in Fig. 3(a)(ii). These plots confirm that the interlaced plasmons are strongly confined inside the slab despite its subwavelength thickness. It is interesting to mention that the normal E_z-field component flips sign within a small layer close to the interface, similar to what happens at optics. In order to achieve the same level of confinement (same value of k_x) in a dielectric waveguide with the same thickness as in the example of Fig. 3(a)(ii), at the normalized frequency $\omega L/c = 0.5$, it would be necessary to use a dielectric with permittivity $\varepsilon_d \approx 130$. The coupling between the two wire grids is particularly strong when the wires make angles $\alpha_1 = 45°$ and $\alpha_2 = -45°$ with respect to the interfaces. It can be verified that if $\alpha_1 = 90°$ and $\alpha_2 = 0°$ the degree of confinement of the guided mode would be significantly reduced.

The previous results assume metals with very high conductivity (PEC). In order to assess the effect of metallic losses and plasmonic effects, we have calculated the propagation constant k_x of the fundamental guided mode at terahertz frequencies for a waveguide with $L = 20$ μm and Ag rods in a selected frequency window [Fig. 3(a)(iii)]. It was assumed that Ag follows the Drude dispersion model, $\varepsilon_m = \varepsilon_\infty - \omega_p^2/(\omega(\omega + i\Gamma))$, with parameters taken from the literature [13]. It is clear from Fig. 3(a)(iii) that the effect of loss is mild in the considered frequency range ($k_x''/k_x' \ll 1$). Moreover, k_x' is nearly unaffected by the metallic losses, since its value is similar to that in the PEC case. In general, the effect of loss is negligible provided the radius of the wires is much larger than the skin depth of metal [10]. In the Supplemental Material [12], it is shown that the interlaced plasmons enable highly confined broadband waveguiding over distances that may exceed the wavelength of operation in the IR regime.

An interesting part of the dispersion diagram corresponds to the regions where $n_{ef} = k_x c/\omega$ varies very steeply. Notice that n_{ef} may be regarded as the effective index of refraction seen by the guided mode. In such branches the group velocity of the mode, $v_g = d\omega/dk_x = c/(n_{ef} + k_0 dn_{ef}/dk_0)$ (with $k_0 = \omega/c$), can be extremely small, and even become negative (backward wave). This property may be interesting for slow light applications in the far infrared. Moreover, also in the wideband regions where $n_{ef} \gg 1$ and n_{ef} varies little with frequency, the group velocity $v_g \approx c/n_{ef}$ can be quite small.

To demonstrate the potential advantages of waveguiding based on interlaced plasmons at terahertz frequencies, next we consider a semiconductor waveguide formed by a slab of indium antimonide (InSb) standing in air. InSb may be described by a Drude dispersion model at terahertz frequencies, and its dielectric response can be tuned by changing the temperature [4]. In Fig. 1(b) we depict the dispersion characteristic [Eq. (3) in Ref. [14]] of the even guided mode in the InSb slab. As shown in Fig. 1(b), in the lossless case (black curve) the air-InSb-air waveguide enables a high field confinement, but over an extremely narrow band as compared to the bandwidth of a crossed wire mesh with the same thickness. Indeed, it is seen in Fig. 3(a)(iii) that the fundamental mode supported by the crossed wires waveguide has $k_x c/\omega \gg 1$ in an dramatically wide band starting at 0.836 THz, whereas the air-InSb-air waveguide enables high field concentration only in the frequency window $0.838 < f\ (\text{THz}) < 0.853$, which corresponds to the spectral region where $\varepsilon_{\text{InSb}} \approx -1$.

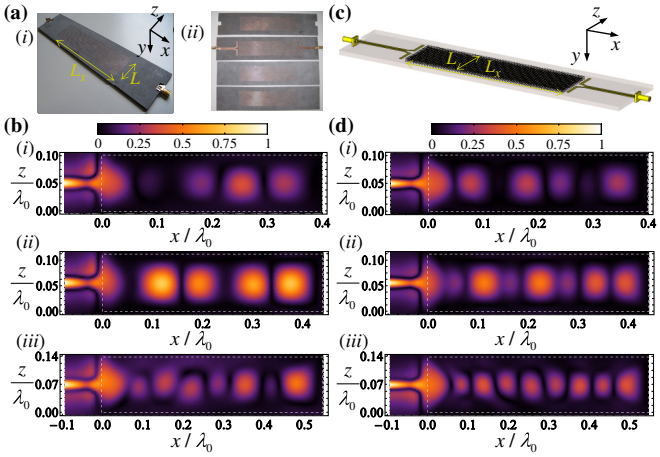

FIG. 4 (color online). (a) Photo of the crossed wires waveguide prototype. (i) General view; (ii) view of the printed boards; the width of the waveguide is $L = 31.48$ mm, the length is $L_x = 4L$, the lattice constant is $a = L/20$, and the width of the metallic strips is $w_s = 0.25$ mm. (b) Normalized measured amplitude of H_y for (i) 950 MHz; (ii) 1.05 GHz; (iii) 1.3 GHz. (c) Crossed wires waveguide as simulated in CST Microwave Studio. (d) The same as in panel (b), but calculated in CST Microwave Studio.

Moreover, when we take into account the material losses (even for an unrealistically small absorption), the field confinement in the InSb-based waveguide decreases drastically, as illustrated in Fig. 1(b). In contrast, the behavior of the interlaced plasmons is weakly sensitive to material losses, as shown in Fig. 3(a)(iii) and in the Supplemental Material [12].

To further validate our theory, and to demonstrate that it is sufficient to consider a few planes of metallic wires, we fabricated a microwave prototype of the crossed wires waveguide using standard printed circuit techniques [Fig. 4(a)]. The proposed structure may be scaled down to shorter wavelengths using nanoimprint techniques. The waveguide is formed by only 4 planes of wires along the y direction. The cylindrical metallic wires are replaced by metallic strips with width $w_s = \pi r_w = \pi a/20 \approx 0.25$ mm, and the host dielectric is RT/duroid 5880, characterized by $\varepsilon_h = 2.2$, loss tangent $\tan\delta \approx 6.5 \times 10^{-4}$, and thickness 0.787 mm. The metamaterial waveguide is excited by a short printed dipole, and the y component of the magnetic field along the waveguide was measured using a near-field scanner with a round shielded loop probe and a vector analyzer (R&S ZVB20). The measured amplitude of H_y is depicted in Fig. 4(b) for different values of frequency (0.95–1.3 GHz). One can see in Fig. 4(b), and also in the time animations [15], that notwithstanding the deeply subwavelength thickness of the slab (of the order of $\lambda/10$), it supports the propagation of strongly confined plasmons. Notice that since the waveguide is not matched to the dipole antennas, in general, the field inside the slab is a standing wave. In Fig. 4(b), as well as in the time animations [15], it can be seen that the magnetic field has even parity, and thus the excited mode is the dominant one [Fig. 3(b)(i)]. In order to validate the experimental results, we have also simulated the response of the metamaterial waveguide using CST Microwave Studio. It can be seen in Fig. 4(d), and also in the time animations [15], that the experimental results are in a quite good agreement with the theory. The small discrepancies may be either related to fabrication imperfections or with deviations in the dielectric substrate permittivity.

In conclusion, it was shown that a crossed wire mesh supports highly confined eigenmodes and a slow light regime, even when the thickness of the waveguide is deeply subwavelength. Such charge density waves are mesoscopic excitations rooted in the strong nonresonant interaction between perpendicular wire grids that support weakly bounded plasmons, and their characteristic spatial period is determined by intrinsic geometrical features rather from the electrical size of the metal dipoles. We compared our crossed wires waveguide with other structures based on spoof plasmons or materials with a plasmonic response at terahertz frequencies, demonstrating the superior potentials of waveguiding based on interlaced plasmons in terms of physical size and bandwidth. The emergence of interlaced plasmons at microwaves was experimentally verified.

M. S. acknowledges useful discussions with C. A. Fernandes, J. R. Costa, and A. Alù.

*tiago.morgado@co.it.pt
†To whom correspondence should be addressed.
mario.silveirinha@co.it.pt

[1] M. Stockman, Phys. Today **64**, No. 2, 39 (2011).
[2] A. V. Akimov *et al.*, Nature (London) **450**, 402 (2007); A. Gonzalez-Tudela *et al.*, Phys. Rev. Lett. **106**, 020501 (2011).
[3] S. A. Maier, *Plasmonics: Fundamentals and Applications* (Springer, New York, 2007); D. K. Gramotnev and S. I. Bozhevolnyi, Nat. Photon. **4**, 83 (2010).
[4] J. G. Rivas *et al.*, Opt. Express **13**, 847 (2005).
[5] S. A. Maier *et al.*, Phys. Rev. Lett. **97**, 176805 (2006).
[6] J. B. Pendry, L. Martín-Moreno, and F. J. Garcia-Vidal, Science **305**, 847 (2004).
[7] A. P. Hibbins, B. R. Evans, and J. R. Sambles, Science **308**, 670 (2005).
[8] S. H. Mousavi *et al.*, Phys. Rev. Lett. **105**, 176803 (2010).
[9] M. Navarro-Cía *et al.*, Opt. Express **17**, 18 184 (2009).
[10] M. G. Silveirinha and C. A. Fernandes, Phys. Rev. B **78**, 033108 (2008).
[11] M. G. Silveirinha, Phys. Rev. Lett. **102**, 193903 (2009).
[12] See Supplemental Material at http://link.aps.org/supplemental/10.1103/PhysRevLett.107.063903 for the analytical model and study of loss.
[13] M. A. Ordal *et al.*, Appl. Opt. **24**, 4493 (1985).
[14] A. Alù and N. Engheta, J. Opt. Soc. Am. B **23**, 571 (2006).
[15] See Supplemental Material at http://link.aps.org/supplemental/10.1103/PhysRevLett.107.063903 for the time animations of H_y for the configurations of Figs. 4(a)–4(d).